



Synthesis of ZnO nano-sono-catalyst for degradation of reactive dye focusing on energy consumption: operational parameters influence, modeling, and optimization

Hiua Daraei^a, Afshin Maleki^{a,*}, Amir Hossein Mahvi^b, Yahya Zandsalimi^a, Loghman Alaei^c, Fardin Gharibi^a

^aEnvironmental Health Research Center, Kurdistan University of Medical Sciences, Sanandaj, Iran
Tel. +98 871 662 5131; email: Maleki_Afshin@ymail.com

^bCenter for Environmental Research, Tehran University of Medical Sciences, Tehran, Iran

^cInstitute of Biochemistry and Biophysics, University of Tehran, Tehran, Iran

Received 9 April 2013; Accepted 26 June 2013

ABSTRACT

Simple synthesized Nano-sized ZnO powder in the absence of high-temperature activation treatments was studied to act as sono-catalyst. Effects of six operational parameters such as initial solution pH (pH_0), initial concentration of dye stuff (C_0), additional dose of nano-sized ZnO powder (D_{SC}), ultrasound (US) irradiation frequency (Fr_{SC}), US irradiation power (P_{SC}), and treatment time (t_{SC}) were examined. Synthetic wastewater containing Reactive Red 198 (RR198) was used as the sample model. Combined design of experiments was done and experiments were conducted according to protocols. The experimental data were collected in a laboratory-scaled batch reactor equipped with ultrasonic bath cleaner as the ultrasonic source. The measured CR% ranging from 0.8 to 100 and EnC (wh) from 0.3 to 13.6 gained under given conditions. The data used for modeling were used in two more common models in this type of studies: Multiple linear regression (MLR) and artificial neural network (ANN). The ANN models obviously outperformed MLR models. Finally, Multi-objective optimization of CR% and EnC was carried out using genetic algorithm (GA) over the outperformed ANN models. The optimization procedure causes non-dominated optimal points which give an insight of the optimal operating conditions.

Keywords: Design of experiments; Artificial neural network; Genetic algorithm multi-objective optimization; Color removal; Sono-catalysis

1. Introduction

Advanced oxidation processes (AOPs) have appeared more appropriate for treating wastewaters containing organic pollutants. In recent years, considerable interest has been drawn to the application of

ultrasound (US) for hazardous chemical destruction. Indeed, sonolysis is a relatively innovative AOP based on the use of low to moderate frequency (typically in the range 20–1,000 kHz) and high energy US to form subsequent collapse of micro-bubbles in a liquid to produce oxidative radicals for the destruction of organic pollutants in aqueous solution. Nevertheless,

*Corresponding author.

the degradation rate via sonolysis is slow and investigations for promoting its efficiency need to be completed [1–3].

More recently, the use of some catalysts such as TiO_2 and ZnO to enhance the efficiency of the US has been known. Indeed, sono-catalytic degradation is a novel technology for wastewater treatment. Compared with photo catalysis, sono-catalysis uses low power ultrasonic irradiation as the exciting energy and can overcome photo catalytic degradation disadvantages. ZnO is a versatile and unique compound with a direct band gap ($E_g=3.37\text{ eV}$) and large exciton binding energy of 60 meV, which has been widely used for its high efficiency, non-toxic nature and low cost. Anju et al. showed that ZnO is very efficient as a sono-catalyst for the destruction of pollutants in aqueous environments. Nevertheless, most of the studies on the sono-catalytic degradation of organic pollutants have been done using TiO_2 catalyst and ZnO has received relatively less attention. Therefore, evaluation of the sono-catalytic properties of ZnO in the decomposition of pollutants is required [4].

No study has been focused on sono-catalytic decomposition of reactive red 198 (RR198) using ZnO by design of experiments (DOE) so far. Recently, DOE has been used to optimize and understand the performance of complex systems with different approaches such as Taguchi method. Dyes are selected as the representative pollutant since they are important classes of aquatic pollutants, which have begun to prove as a major source of environmental contamination. Because the presence of trace amounts of dyes (less than 1 ppm for some dyes) is highly visible and influences water quality considerably and unfortunately, they are usually neutralized into water bodies without complete treatment. Hence, removal of dyes from those effluents is one of the most significant environmental problems [3,5–8].

Therefore, the aim of this work is to synthesise nano-sized ZnO as a sono-catalyst with high catalytic activity for decomposition of reactive red 198 as the representative common dye, which has lots of applications in textile dyeing industries. In addition, some operational factors influencing the increase of color removal efficiency and decrease of energy consumption (EC) were also studied using Genetic Algorithm (GA) based on artificial neural network (ANN) model.

2. Materials and methods

2.1. Materials

Zinc acetate ($\text{Zn}(\text{CH}_3\text{COO})_2 \cdot 2\text{H}_2\text{O}$), as a precursor of the nano-sized ZnO powder, was of analytical

grade and purchased from Merck. Reactive red 198 ($\text{C}_{27}\text{H}_{18}\text{ClN}_7\text{Na}_4\text{O}_{15}\text{S}_5$) was obtained from Alvan Sabet dye manufacturing industry located in Hamedan, Iran. All other chemicals were purchased from Merck Chemical Co., and used without further purification. All solutions were prepared fresh by distilled water.

2.2. Instruments

UV–vis spectrometer (DR-5000, Perkin–Elmer Company, USA) was used to chase the sono-catalytic degradation process of reactive red 198. Total organic carbon (TOC) was measured using a TOC Analyzer (Skalar, The Netherlands). Sonication was done at frequencies of 37 and 80 kHz with an ultrasonic generator (Elmasonic P30H, Germany) with a piezoelectric transducer fixed at the bottom of the vessel. Effective ultrasonic powers of the ultrasonic generator were 100 W. Ultrasonic intensity is adjustable from 40 to 100% in increments of 20% of effective ultrasonic powers.

2.3. Nano-sono-catalyst preparation

Precipitation method was used for ZnO nano-sono-catalyst preparation. For this purpose, 6 g of zinc acetate was dissolved in 100 ml of 0.1 N NaOH solution under vigorous stirring at room temperature and subsequently 40 ml of deionized water was added to the above solution under continuous stirring for 24 h. Afterwards, the mixture was centrifuged, washed with deionized water several times, and dried at 100°C for 12 h. Finally, ZnO nano particles were collected and stored in a desiccator for further experimental studies.

2.4. Methodology of nano-sono-catalyst characterization

The synthesized nano particles were characterized using X-ray diffraction (XRD, D_8 Advance, Bruker, Germany), Fourier transform infrared spectroscopy (Tensor 27 spectrophotometer, Bruker Optic, GmbH, Germany), scanning electron microscopy (SEM, JOEL Ltd., Tokyo, Japan), energy dispersive spectroscopy (EDS, Genesis 30T), zeta potential, and particles size analyzer (Zetasizer-2000, Malvern instruments).

2.5. Experimental design

The experimental conditions including the initial dye concentration (C_0) of 20–200 mg/L at four levels, catalyst dose (D_{SC}) of 0.1–2 mg/L at four levels, pH value of 3–11 at four levels, US frequency (Fr_{SC}) at two levels, and ultrasonic power (P_{SC}) at four levels

were selected for evaluation of sono-catalytic activity. The combined design of Taguchi for C_0 , D_{SC} , pH_0 , Fr_{SC} , P_{SC} , and full factorial for reaction time (t_{SC}) was used to design the experiments using Minitab 14. A Combined DOE was selected due to the complex kinetics of the sono-catalysis reaction and the need to more complete t_{SC} data-set [9]. The Taguchi was designed based on an L_{32} orthogonal array with five factors. The experiments were done randomly to avoid noise sources, which may take place during an experiment. In these 32 experiments, seven levels of t_{SC} were determined. All the selected experimental conditions can be seen in Fig. 2.

2.6. Procedure and analytical methods

The reaction volume was 200 and studies were carried out for 90 min at seven levels. The experiments were performed by mixing ZnO with reactive red 198 solutions. Then, each suspension was irrigated and after certain intervals, samples were taken for analysis. The color removal efficiency (CR%) was calculated for the decanted solutions. The color of the solution was evaluated at the maximum wavelength (λ_{max}). The λ_{max} of each solution in special conditions was determined using one spectra analysis on zero time reference samples to prevent the matrix effect on maximum wavelength. The CR% was calculated for each sample using Eq. (1):

$$CR\% = \left(1 - \frac{A}{A_0}\right) \times 100 \quad (1)$$

where A_0 and A are absorptions of the solution before and after the process, respectively. Furthermore, the EC of ultrasonic process (EC) was calculated for each sample using the information reported by the company of ultrasonic unit as follows (Eq. (2)):

$$EPM = \left[p \times \left(\frac{V}{V_T} \right) \times t_{us} \right] / (CR\% \times C_0 \times V) \quad (2)$$

where P_{SC} is the power of the sonicator unit (Watt), V is the effective volume of the reactor (Liter), V_T is the total volume of the ultrasonic bath (Liter), and t_{SC} is the treatment time (h).

2.7. Methodology of modeling

The 224 obtained values for CR% and EC together with the corresponding experimental conditions were used to make a data-set. The six operational parameters were applied as inputs of multiple linear

regression (MLR) and ANN models whilst the CR% and EC were considered as dependent variables. Data-set was randomly divided into three parts; 60% as training set, 20% as validation set, and 20% as testing set. The MLR and ANN models were constructed based on the same data-sets for both CR% and EC, separately. Back propagation algorithm was used in this study as it is very fast and can be employed quite easily. The optimum parameters for ANN models especially the number of hidden layers and the number of neurons were determined via a trial and error procedure [10–14].

2.8. Methodology of GA multi-objective optimization

Optimization of CR% and EC falls in the field of multi-objective optimization. There is no matchless solution to this type of optimization problem, but a set of mathematically equal solutions known as Pareto optimal solutions. GA toolbox in MATLAB (version 7) was used for generating the Pareto optimal solutions for CR% and EC using “gamultiobj” function. MATLAB functions were written using ANN model as the inputs for creating a fitness function for the multi-objective optimization problem. The CR% component to be maximized was negated in the vector-valued fitness function since “gamultiobj” minimizes all the objectives. Experimental ranges were placed as bounds on the six inputs [12,13].

3. Results and discussions

3.1. Nano-ZnO characterization

Particle size analysis was used to determine the ZnO powder size and its distribution. The results showed that the average size is 888 nm and the particles are uniform with low size distribution (Fig. 1). SEM was used to describe the shape and size of nano-sized ZnO particles. From Fig. 2, it is found that the nano-sized ZnO powders are agglomerated and are of a nanometer scale with the size around 800 nm. Hence, the average size determined by size distribution analysis (888 nm) was in good agreement with the size observed by SEM.

Zeta potential analysis was used to determine the surface potential of nano particles that controls the stability of particles in water media. The results show the zeta potential to be equal to 8.59 mv. This range of zeta potential belongs to low stable particles in water media. However, this result is not promising for a photocatalyst particle, but it is not concerning for sono-catalyst particles in the presence of permanent ultrasonic irradiation.

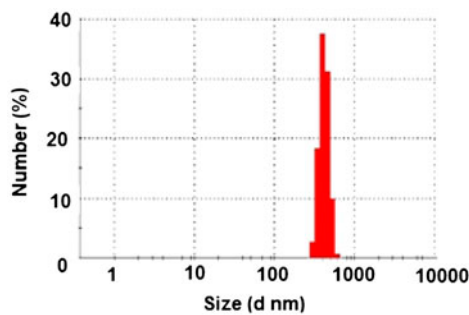


Fig. 1. Particle size distribution of nano ZnO particles.

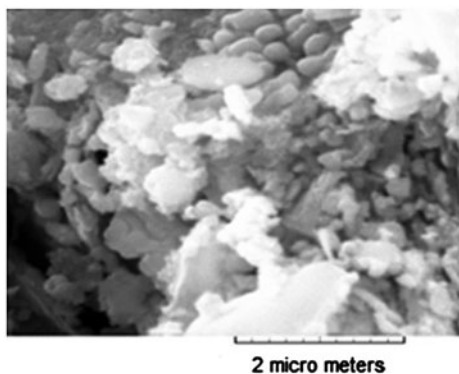


Fig. 2. SEM image of nano ZnO particles.

Finally, the XRD and EDX analyses were used to confirm the crystalline structure and purity of ZnO nano particles. These results show up to 99.6% purity with less than 0.4% Cu impurity. The XRD spectrum was compared with the standard spectrum for ZnO that showed good agreement (Fig. 3). Less intense, crowded baseline, and extra peaks are because of two reasons: first, the synthesis was done without any calcinations and second, the presence of copper impurity [15].

The UV–vis spectra were used for energy gap determination. The spectra were recorded in two solvents: water and ethanol. The calculated values for energy gap were 3.41 and 3.39 eV for nano ZnO particles in water and ethanol, respectively.

Fig. 4 shows the FT-IR absorption spectrum of ZnO nano particles. The broad peak at 3400 cm^{-1} is attributed to the characteristic absorption of hydroxyl radicals. Peaks at about 1550 and 1350 cm^{-1} are due to the stretching vibrations of C=O group. The peak at 450 cm^{-1} is the characteristic absorption band of ZnO.

3.2. Sono-catalysis process

Table 1 contains the whole 224 CR% and ECs, obtained in all of the experiment conditions. Table 1

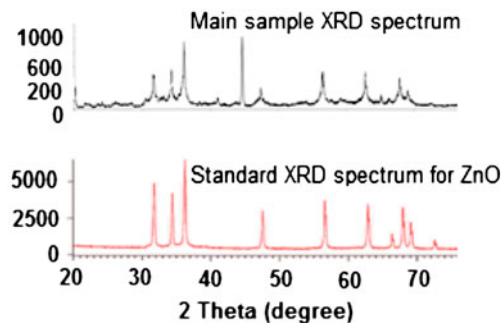


Fig. 3. XRD spectra of synthesized and standard ZnO nano particles.

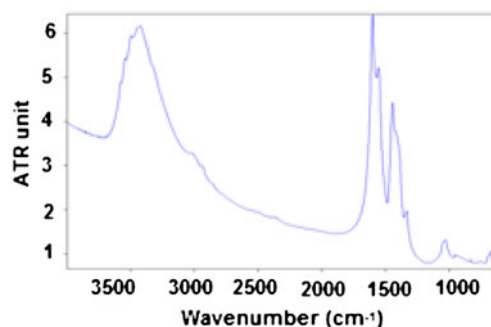


Fig. 4. FT-IR spectra of prepared ZnO.

clearly shows that different levels of experimental parameters result in different CR% and EC. In addition, it was found that the nano-sized ZnO powder is propitious in enhancing the ratios of CR% as a sono-catalyst.

3.3. Mineralization studies using TOC and UV–vis spectra

Decay of TOC reflects the extent of mineralization of an organic compound, and the reduction percent of TOC was studied for dye samples ($C_0=200\text{ mg/L}$, $D_{SC}=2\text{ g/L}$, $P_{SC}=80\text{ w}$, $\text{pH}=\text{natural}$, $Fr_{SC}=80\text{ kHz}$) as a function of the sonication time. The control sample was considered to compensate residual acetate TOC of nano zinc oxide. It was observed that the TOC reduction percent lies between 710 and 925 for time 20 and 120 min for the main sample and 211 and 177 for the control samples (Fig. 5). Both spectroscopy and TOC analyses showed that at the $t_{SC}=90\text{ min}$, degradation and color fading was complete. It means that the results of TOC are in accordance with spectroscopy analysis. The increase of TOC in the control sample is due to the ultrasonic irradiation that stimulates the release of residual organic materials like acetate from the surface and the pores of nano particles. The results for TOC show less removal rather than

Table 1
Whole 224 CR% and EC dataset

Empirical conditions						Time (min)						
						5	10	20	30	45	60	90
No.	Fr _{SC}	P _{SC}	pH ₀	C ₀	D _{SC}	CR%	EC					
1	37	40	3	20	0.1	7.47	18.07	19.04	20	20.48	22.17	28.92
						0.3	0.61	1.21	1.82	2.73	3.64	5.45
2	37	40	6	80	0.9	72.35	84.94	87.04	88.15	89.44	89.57	71.67
						0.3	0.61	1.21	1.82	2.73	3.64	5.45
3	37	40	9	140	1.4	26.7	42.87	47.43	51.34	54.21	57.05	57.66
						0.3	0.61	1.21	1.82	2.73	3.64	5.45
4	37	40	11	200	2	7.79	10.85	12.23	20.14	22.92	56.07	78.89
						0.3	0.61	1.21	1.82	2.73	3.64	5.45
5	37	60	3	20	0.9	97.85	97.85	98.8	99.04	99.52	99.76	99.76
						0.45	0.91	1.82	2.73	4.09	5.45	8.18
6	37	60	6	80	0.1	5.63	8.08	8.8	8.92	8.92	10.29	12.33
						0.45	0.91	1.82	2.73	4.09	5.45	8.18
7	37	60	9	140	2	80.01	87.12	96.17	96.17	96.25	96.36	96.5
						0.45	0.91	1.82	2.73	4.09	5.45	8.18
8	37	60	11	200	1.4	38.23	39.69	40.15	40.35	40.64	40.67	41.24
						0.45	0.91	1.82	2.73	4.09	5.45	8.18
9	37	80	3	80	1.4	85.78	89.06	92.23	93.11	93.36	94.18	94.63
						0.61	1.21	2.42	3.64	5.45	7.27	10.91
10	37	80	6	20	2	98.64	99.09	99.32	99.55	99.77	99.77	100
						0.61	1.21	2.42	3.64	5.45	7.27	10.91
11	37	80	9	200	0.1	1.05	1.92	1.98	2.24	2.36	2.48	3.12
						0.61	1.21	2.42	3.64	5.45	7.27	10.91
12	37	80	11	140	0.9	23.73	38.1	40.61	40.65	40.34	40.84	41.33
						0.61	1.21	2.42	3.64	5.45	7.27	10.91
13	37	100	3	80	2	96.08	98.71	99.02	99.45	99.82	99.82	99.88
						0.76	1.52	3.03	4.55	6.82	9.09	13.64
14	37	100	6	20	1.4	98.49	99.35	99.35	99.57	99.78	100	100
						0.76	1.52	3.03	4.55	6.82	9.09	13.64
15	37	100	9	200	0.9	11.83	12.21	12.3	12.39	12.66	12.66	12.72
						0.76	1.52	3.03	4.55	6.82	9.09	13.64
16	37	100	11	140	0.1	2.85	3.04	3.08	3.31	3.31	3.39	3.42
						0.76	1.52	3.03	4.55	6.82	9.09	13.64
17	80	40	3	200	0.1	2.11	3.51	3.75	10.2	5.41	5.43	7.76
						0.3	0.61	1.21	1.82	2.73	3.64	5.45
18	80	40	6	140	0.9	24	26.21	27.42	29.44	30.77	31.91	32.2
						0.3	0.61	1.21	1.82	2.73	3.64	5.45
19	80	40	9	80	1.4	93.63	94.28	95.59	96.46	96.9	97.17	97.55
						0.3	0.61	1.21	1.82	2.73	3.64	5.45
20	80	40	11	20	2	99.52	99.52	99.52	99.76	99.76	99.76	99.76
						0.3	0.61	1.21	1.82	2.73	3.64	5.45
21	80	60	3	200	0.9	3.9	3.9	4.73	4.77	6.5	6.97	9.17
						0.45	0.91	1.82	2.73	4.09	5.45	8.18
22	80	60	6	140	0.1	3.11	6.82	6.93	7.35	8.18	8.37	9.81
						0.45	0.91	1.82	2.73	4.09	5.45	8.18

(Continued)

Table 1
(Continued)

Empirical conditions						Time (min)						
						5	10	20	30	45	60	90
No.	Fr _{SC}	P _{SC}	pH ₀	C ₀	D _{SC}	CR%	EC					
23	80	60	9	80	2	41.04	63.96	79.33	87.13	88.6	93.17	94.76
						0.45	0.91	1.82	2.73	4.09	5.45	8.18
24	80	60	11	20	1.4	97.06	97.59	98.93	99.2	99.47	99.73	99.73
						0.45	0.91	1.82	2.73	4.09	5.45	8.18
25	80	80	3	140	1.4	5.92	9.64	29.94	38.17	58.4	67.81	78.58
						0.61	1.21	2.42	3.64	5.45	7.27	10.91
26	80	80	6	200	2	25.85	40.4	61.51	71.29	89.75	97.14	98.52
						0.61	1.21	2.42	3.64	5.45	7.27	10.91
27	80	80	9	20	0.1	18.14	21	21.24	22.91	27.21	27.68	32.46
						0.61	1.21	2.42	3.64	5.45	7.27	10.91
28	80	80	11	80	0.9	0.28	0.64	0.92	2.2	2.84	3.63	48.44
						0.61	1.21	2.42	3.64	5.45	7.27	10.91
29	80	100	3	140	2	24.19	38.53	62.42	74.44	80.96	84.68	89.46
						0.76	1.52	3.03	4.55	6.82	9.09	13.64
30	80	100	6	200	1.4	9.89	17.23	17.39	31.54	35.28	37.57	39.23
						0.76	1.52	3.03	4.55	6.82	9.09	13.64
31	80	100	9	20	0.9	98.4	98.86	99.09	99.32	99.54	99.77	99.77
						0.76	1.52	3.03	4.55	6.82	9.09	13.64
32	80	100	11	80	0.1	0.65	0.65	0.85	2.16	3.01	5.1	8.24
						0.76	1.52	3.03	4.55	6.82	9.09	13.64

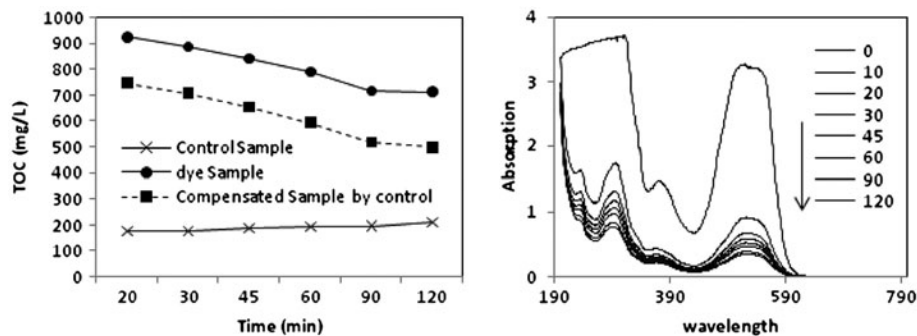


Fig. 5. TOC samples and absorption removal during SC for main and control samples at $C_0=200$ mg/L, $D_{SC}=2$ g/L, $p=80$ w, pH = natural, Fr_{SC} = 80 kHz.

spectroscopy. It shows that decolorization can happen when the mineralization of the compound did not complete and only degradation takes place.

Fig. 5 also shows the UV–Vis spectra of RR198 under the same TOC experiment conditions. It was found that the absorption peaks of RR198 solutions declined under ultrasonic irradiation in the presence of nano-sized ZnO powder. It indicates that RR198 is mostly degraded and disappeared gradually in aqueous solution.

3.4. MLR models

Two MLR models were separately developed for CR% and EC [12,13]. Both the models and the corresponding statistical characteristics are given in Table 2.

Based on unbiased standardized coefficients presented in Table 2, among linear parameters, C_0 , Fr_{SC}, and pH₀ have negative effect, but D_{SC} and t_{SC} have positive effects on CR%. The most important

parameters were D_{SC} and pH_0 . Table 2 indicates that the MLR model does not have good predictability for CR% due to the complex mechanism of the sorption process. It demonstrates new interest in using more powerful modeling approaches especially ANN model [12].

3.5. ANN model

The best ANN models were separately constructed for each CR% and EC. For both CR% and EC models, one hidden layer with 8 neurons and 0.15 learning rate were applied. The “tansig” transfer function was selected for input and hidden layers and “purelin” for output in both models [10,11]. Once the networks

trained, the weights and bias of each neuron and layer were saved in the ANN model. Then, they were used to estimate the test set. The (6:8:1) ANN for CR% and EC was trained using 134 data of the train set by back propagation algorithm. Tables 3 and 4 present the parameters of ANN models for CR% and EC, respectively.

Moreover, Fig. 6 shows the samples of ANN and MLR predictions and their corresponding experimental results for CR%.

Statistical goodness parameters of ANN models collected in Table 5. A glance at Fig. 6 and comparison of Tables 2 with 5 clearly shows that ANN models outperformed MLR models. Therefore, ANN models would be used in optimization procedure by GA.

Table 2
Statistical characteristics of MLR models of CR% and EC

Model	CR%			EC (wh)		
	Coeff.	St. coeff.	p-value	Coeff.	St. coeff.	p-value
Constant	50.303	8.792	0	-4.09	0.451	0
pH_0	-0.622	0.537	0.025	-0.01	0.028	0.726
C_0	-0.298	0.024	0	0	0.001	0.894
Fr_{SC}	-0.140	0.076	0.068	-0.003	0.004	0.452
D_{SC}	37.023	2.317	0	0.122	0.119	0.307
P_{SC}	-0.030	0.072	0.68	0.057	0.004	0
t_{SC}	0.200	0.058	0.001	0.111	0.003	0
Data set	Train (75 data)		Test (51 data)	Train set (64)		Test set (44)
R^2	0.77		0.77	0.93		0.91
RMSE	18.0		19.6	3.8		0.99

Table 3
Network weights and biases of the ANN model for CR%

Neuron	Input layer to hidden layer weights						Bias		
	pH_0	C_0	Fr_{SC}	D_{SC}	P_{SC}	t_{SC}			
n_1	2.26	-0.23	-1.39	-1.23	0.01	-0.72	-2.19		
n_2	-1.17	-0.58	0.87	-1.71	-2.38	-0.81	1.91		
n_3	0.94	-1.39	-0.64	3.58	-0.47	0.04	1.15		
n_4	-1.32	1.83	1.27	0.78	-0.73	-0.43	-0.68		
n_5	0.72	0.08	1.40	1.62	0.83	-0.64	-0.02		
n_6	1.12	-0.07	0.41	0.73	1.86	-0.59	-0.41		
n_7	1.42	0.04	0.00	-0.88	1.34	1.24	1.69		
n_8	0.34	-0.82	1.26	-0.54	0.69	-0.89	2.29		
Hidden layer to output layer weights									
Output	n_1	n_2	n_3	n_4	n_5	n_6	n_7	n_8	Bias
	-0.98	-0.54	1.24	-0.76	0.68	-0.97	0.49	1.21	2.073

Note: n : Neuron or processing elements.

Table 4
Network weights and biases of the ANN model for EC

Neuron	Input layer to hidden layer weights						Bias
	pH ₀	C ₀	Fr _{SC}	D _{SC}	P _{SC}	t _{SC}	
n1	0.004	0.001	−0.003	−0.001	−0.278	0.351	−0.94
n2	0.002	−0.008	−0.009	0.005	0.163	4.871	5.77
n3	0.003	0.000	−1.239	0.002	0.034	0.615	−0.22
n4	0.522	0.600	−0.562	0.992	−2.425	2.572	0.72
n5	−2.524	0.493	0.996	0.953	0.238	−1.224	−0.99
n6	−0.704	−0.654	0.666	−0.482	2.194	−0.065	−0.68
n7	0.010	−0.001	−0.013	0.004	−2.534	−2.941	5.61
n8	−0.004	0.000	−1.151	0.001	−0.039	−0.577	0.20

Output	Hidden layer to output layer weights								Bias
	n1	n2	n3	n4	n5	n6	n7	n8	
	−2.26	2.45	2.90	−0.01	0.00	−0.01	−2.95	−2.99	−1.06

Note: *n*: Neuron or processing elements.

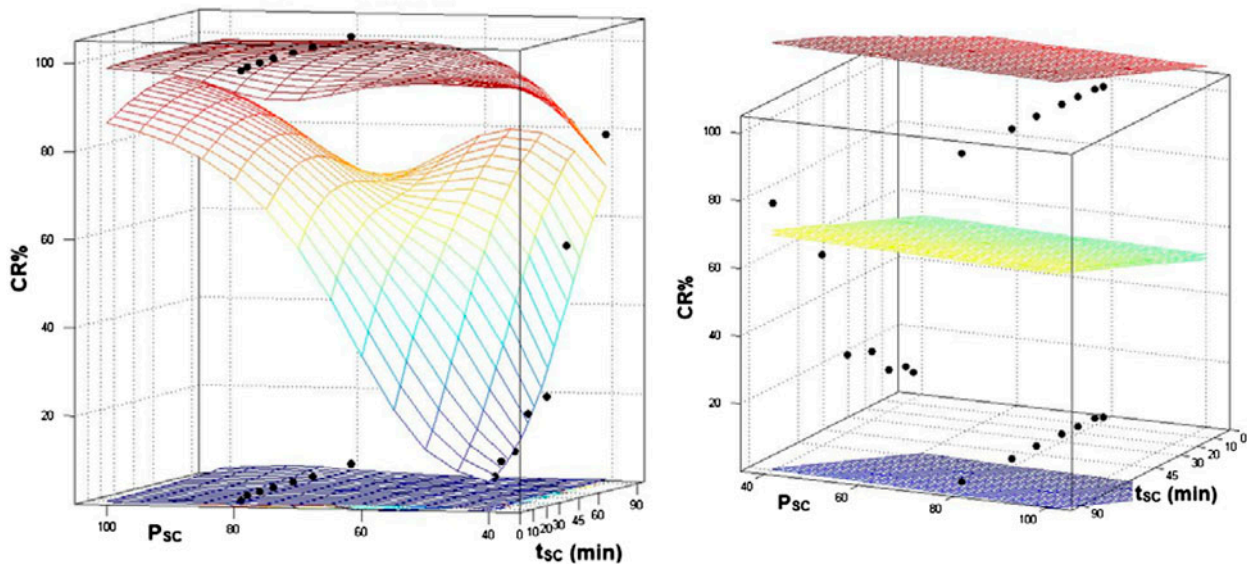


Fig. 6. Samples plot (Run 4, 10, and 11) of the ANN (left) and MLR (right) predicted values of CR% (surface) vs. experimental data of CR% (dotes), for three conditions, (a) pH₀=9, C₀=200 mg/L, Fr_{SC}=37 kHz and D_{SC}=0.1 g/L (down diagram); (b) pH₀=11, C₀=200 mg/L, Fr_{SC}=37 kHz and D_{SC}=2 g/L (middle diagram); (c) pH₀=6, C₀=20 mg/L, Fr_{SC}=37 kHz and D_{SC}=2 g/L (up diagram).

3.6. GA multi-objective optimization

Multi-objective optimization process results a Pareto-optimal solutions set. Each point on the Pareto set is associated with a set of decision variables. Moreover, the input decision variables corresponding to each of the Pareto optimal solutions are tabulated in Table 6. Interpretation of Tables 2 and 6 was used to discriminate the effect of each investigated parameter.

3.7. Effect of solution pH₀ on the CR% and EC

It is well known, generally, that the pH₀ values markedly influence the degradation of organic pollutants in sono-catalytic degradation reaction. Then, the effect of pH₀ values was studied at four levels in the range of 3–11 on the sono-catalytic degradation. As can be seen from Table 6, the optimum value of pH₀ in all Pareto-optimal solutions is in the range of 7–8.

In general, the point of zero charge (PZC) of nano ZnO powder is around pH=9. Above this pH, the surface of nano ZnO particles is negatively charged, while below this pH it is positively charged. Some ionizable compounds like RR198 (negatively charged) after ionization can be easily adsorbed on the positively charged surface of nano-sized particles below pH=9, which is propitious for the degradation of RR198. While in basic medium, the adsorption ability of nano ZnO powder decreases for RR198 having a negative charge.

3.8. Effect of C_0 on the CR% and EC

Four different initial concentrations of RR198 solutions ranging from 20.0 to 200.0 mg/L were used to study its influence on the CR% and EC. As presented in Table 6, the optimum value of C_0 is in the range of 35–87 mg/L. The increase in CR% with increase in C_0 until about 90 mg/L is in accordance with the nature of this kind of process kinetics. But for the decrease in CR% up to 90 mg/lit two reasons can be presented: First, the adsorption amounts of nano ZnO powder

attain saturation for superfluous RR198. Second, the mutual screens among the RR198 molecules also increase along with the rising concentration of RR198.

3.9. Effect of Fr_{SC} on the CR% and EC

The influence of ultrasonic frequency on the CR% of RR198 was studied using two different 37 and 80 kHz frequencies. The optimum value of Fr_{SC} was almost 50 kHz (Table 6).

3.10. Effect of D_{SC} on the CR% and EC

Table 2 shows the influence of D_{SC} on the CR% and EC. The experiments with different D_{SC} showed that the sono-catalytic degradation trend of RR198 tremendously increases with the increase of nano-sized ZnO powder from 0.1 mg/L to up to 0.9 g/L. The optimum value of D_{SC} was almost 1.4–1.9 g/L (Table 6). More D_{SC} caused mutual screens among nano ZnO particles, which results in the decrease of the sono-catalytic activity of ZnO nano-powder.

3.11. Effect of P_{SC} on CR% and EC

In general, the CR% should increase with increasing P_{SC} with or without sono-catalyst. It may have two causes: first, high output power provides more hydroxyl radicals because of more cavities and more energy offered to ZnO catalyst. Second, the nano ZnO particles can retain stable dispersed particles of a suitable size. Based on the optimization process results, the optimum values for P_{SC} were 43 and 100 W, in all

Table 5
Statistical characteristics of both ANN models for CR% and EC

Model	CR%			EC (wh)		
	Train	Validation	Test	Train	Validation	Test
R^2	0.986	0.982	0.98	1	0.999	0.999
RMSE	4.8	5.8	5.7	0.02	0.03	0.04

Table 6
Variable values corresponding to each of the Pareto-optimal solution

Solutions	pH ₀	C ₀	Fr _{SC}	D _{SC}	P _{SC}	t _{SC}	CR%	EC	Solutions	pH ₀	C ₀	Fr _{SC}	D _{SC}	P _{SC}	t _{SC}	CR%	EC
1	7.5	83	58.2	1.7	100	>1	99.2	0.30	15	8.5	82	58.2	1.7	100	>1	99.3	0.30
2	8.5	83	58.2	1.9	100	>1	99.4	0.30	16	8.5	82	58.7	1.4	42	>1	95.7	0.30
3	7.0	83	58.2	1.4	100	>1	98.5	0.30	17	7.7	40	58.4	1.4	42	>1	98.0	0.30
4	7.5	83	58.2	1.5	100	>1	99.0	0.30	18	7.5	83	58.4	1.4	100	>1	99.5	0.31
5	6.9	35	58.7	1.9	100	3	99.7	0.31	19	7.0	83	58.2	1.4	100	>1	98.5	0.30
6	6.9	35	58.7	1.9	100	2	99.7	0.31	20	7.7	57	58.2	1.5	42	>1	97.4	0.30
7	8.5	83	58.2	1.4	100	>1	98.8	0.30	21	6.9	35	58.4	1.9	100	3	99.7	0.31
8	7.7	35	58.7	1.5	42	>1	98.2	0.30	22	8.5	40	58.4	1.4	42	>1	97.6	0.30
9	6.9	36	58.4	1.9	100	2	99.7	0.31	23	8.5	82	58.4	1.4	42	>1	95.7	0.30
10	7.7	35	58.7	1.4	42	>1	98.1	0.30	24	8.5	82	58.4	1.5	100	>1	99.1	0.30
11	6.9	35	58.6	1.9	100	>1	99.7	0.31	25	7.7	40	58.4	1.4	42	>1	98.0	0.30
12	7.7	35	58.7	1.5	42	3	98.3	0.30	26	8.5	57	58.4	1.4	42	>1	97.2	0.30
13	8.5	57	58.4	1.4	42	>1	97.2	0.30	27	7.5	83	58.2	1.4	100	>1	98.7	0.30
14	8.5	83	58.4	1.4	42	>1	95.6	0.30	28	8.5	40	58.4	1.4	42	>1	97.6	0.30

conditions. It can be said that, optimization of EnC caused to optimum P_{SC} value less than 100 W. It is obvious that if more power needs more EC, then the optimum value was selected based on both parameters.

3.12. Effect of t_{SC} on CR% and EC

Table 2 shows the comparison of CR% and EC at different times. It can be seen that the CR% of RR198 solutions gradually increased along with t_{SC} increasing, which indicates that RR198 degraded steadily in aqueous solutions under ultrasonic irradiation. In contrast, Table 6 shows that optimum t_{SC} is less than 3 min that is because of energy saving in minimum t_{SC} .

3.13. Possible sono-catalytic removal process and its mechanism

There has been no certain mechanism and satisfying explanation yet on the sono-catalytic degradation of organic pollutants in the presence of various semiconductor materials. But, the two hypotheses have been presented as the more logical statements to explain the process. Firstly, it has been well known that the ultrasonic irradiation can result in the formation of the light with a comparatively wide wavelength range. These wavelengths are below 375 nm, beyond all doubt, and can excite the nano-sized ZnO particle, acting as a photo-catalyst and forming great deals of hydroxyl radicals with high oxidative activity on the surface of the nano-sized ZnO particles. Secondly, the temperature named "hotspot" produced by ultrasonic activation in water medium can achieve 10^5 or 10^6 °C, such a high-temperature sufficiently brings many holes producing hydroxyl radicals on the surface of nano-sized ZnO particles. Of course, the detailed mechanism is expected to be further and specially studied [16].

4. Conclusion

The experimental conditions including the initial dye concentration (C_0) of 20–200 mg/L at four levels, catalyst dose (D_{SC}) of 0.1–2 mg/L at four levels, pH value of 3–11 at four levels, US frequency (Fr_{SC}) at two levels, and ultrasonic power (P_{SC}) at four levels were selected for evaluation of sono-catalytic activity. RR198 aqueous solutions can be obviously discolored and degraded by sono-catalytic technique in the presence of synthesized nano-sized ZnO powder. The CR% (0.8–100) and EnC (wh) (0.3–13.6) gained under experimental conditions. The data were used for

modeling by employing two more popular models in these kinds of studies: MLR and ANN. The ANN models obviously outperformed the MLR models. Finally, multi-objective optimization of CR% and EnC was carried out using GA over the outperformed ANN models. The optimization procedure causes non-dominated optimal points which gave an insight of the optimal operating conditions. The multi-objective optimal conditions were as: pH_0 , 7–8, C_0 , 35–87 mg/L, D_{SC} , 1.4–1.9 g/L, Fr_{SC} , 58 kHz and P_{SC} , 43 and 100 W.

Acknowledgment

The authors greatly acknowledge The Kurdistan Environmental Health Research Center, Sanandaj Branch, for their financial supports, laboratory, and material preparation.

Symbols

CR%	—	color removal efficiency, percent
pH_0	—	initial pH of dye solution
P_{SC}	—	applied power, Watt
C_0	—	initial dye concentration, mg L ⁻¹
D_{SC}	—	dose of dissolved sono-catalyst
Fr_{SC}	—	applied frequency, kHz
t_{SC}	—	treatment time, minute
EC	—	energy consumption per mass, wh/g
A_0	—	initial absorbance of dye solution
A	—	absorbance of solution after SC

References

- [1] W.J. Cooper, C.J. Cramer, N.H. Martin, S.P. Mezyk, K.E. O'Shea, C. von Sonntag, Free radical mechanisms for the treatment of methyl tert-butyl ether (MTBE) via advanced oxidation/reductive processes in aqueous solutions, *Chem. Rev.* 109 (2009) 1302–1345.
- [2] A. Maleki, A.H. Mahvi, R. Ebrahimi, Y. Zandsalimi, Study of photochemical and sonochemical processes efficiency for degradation of dyes in aqueous solution, *Korean J. Chem. Eng.* 27 (2010) 1805–1810.
- [3] A.H. Mahvi, A. Maleki, Photosonochemical degradation of phenol in water, *Desalin. Water Treat.* 20 (2010) 197–202.
- [4] S. Anju, K. Jyothi, S.Y. Sindhu Joseph, E. Yesodharan, Ultrasound assisted semiconductor mediated catalytic degradation of organic pollutants in water: Comparative efficacy of ZnO, TiO₂ and ZnO-TiO₂, *Res. J. Rec. Sci.* 1 (2012) 191–201.
- [5] S. Venkata Mohan, N. Chandrasekhara Rao, K. Krishna Prasad, P. Murali Krishna, R. Sreenivas Rao, P. Sarma, Anaerobic treatment of complex chemical wastewater in a sequencing batch biofilm reactor: Process optimization and evaluation of factor interactions using the Taguchi dynamic DOE methodology, *Biotechnol. Bioeng.* 90 (2005) 732–745.

- [6] S. Kovarich, E. Papa, P. Gramatica, QSAR classification models for the prediction of endocrine disrupting activity of brominated flame retardants, *J. Hazard. Mater.* 190 (2011) 106–112.
- [7] M. Landi, V. Naddeo, V. Belgiorno, Influence of ultrasound on phenol removal by adsorption on granular activated carbon, *Desalin. Water Treat.* 23 (2010) 181–186.
- [8] J.-S. Park, N. Her, Y. Yoon, Ultrasonic degradation of bisphenol A, 17 β -estradiol, and 17 α -ethinyl, *Desalin. Water Treat.* 30 (2011) 300–309.
- [9] D.M. Himmelblau, Applications of artificial neural networks in chemical engineering, *Korean J. Chem. Eng.* 17 (2000) 373–392.
- [10] H. Daraei, M. Irandoust, J.B. Ghasemi, A.R. Kurdian, QSPR probing of Na⁺ complexation with 15-crown-5 ethers derivatives using artificial neural network and multiple linear regression, *J. Incl. Phenom. Macro.* 72 (2011) 423–435.
- [11] T. Hatami, M. Rahimi, H. Daraei, E. Heidaryan, A.A. Alsairafi, PRSV equation of state parameter modeling through artificial neural network and adaptive network-based fuzzy inference system, *Korean J. Chem. Eng.* 29 (2012) 657–667.
- [12] M.S. Bhatti, D. Kapoor, R.K. Kalia, A.S. Reddy, A.K. Thukral, RSM and ANN modeling for electrocoagulation of copper from simulated wastewater: Multi objective optimization using genetic algorithm approach, *Desalination* 274 (2011) 74–80.
- [13] Y. Safa, H.N. Bhatti, Adsorptive removal of direct textile dyes by low cost agricultural waste: Application of factorial design analysis, *Chem. Eng. J.* 167 (2011) 35–41.
- [14] S.P. Niculescu, Artificial neural networks and genetic algorithms in QSAR, *J. Mol. Struct. Theochem.* 622 (2003) 71–83.
- [15] C.K. Srikanth, P. Jeevanandam, Effect of anion on the homogeneous precipitation of precursors and their thermal decomposition to zinc oxide, *J. Alloys Compd.* 486 (2009) 677–684.
- [16] J. Wang, T. Ma, Z. Zhang, X. Zhang, Y. Jiang, Z. Pan, F. Wen, P. Kang, P. Zhang, Investigation on the sonocatalytic degradation of methyl orange in the presence of nanometer anatase and rutile TiO₂ powders and comparison of their sonocatalytic activities, *Desalination* 195 (2006) 294–305.